# High-flux monochromatic ion and electron beams based on laser-cooled atoms

L. Kime,[1,2] A. Fioretti,[1,4,5] Y. Bruneau,[1] N. Porfido,[4] F. Fuso,[4] M. Viteau,[2] G. Khalili,[1] N. Šantić,[1] A. Gloter,[3] B. Rasser,[2] P. Sudraud,[2] P. Pillet,[1] and D. Comparat[1]

[1]*Laboratoire Aimé Cotton, CNRS, Université Paris-Sud, ENS Cachan, Bât. 505, 91405 Orsay, France*
[2]*Orsay Physics, 95 Avenue des Monts Auréliens, ZA Saint-Charles, 13710 Fuveau, France*
[3]*Laboratoire de Physique des Solides, UMR 8502, Université Paris-Sud, Bât. 510, 91405 Orsay, France*
[4]*Dipartimento di Fisica, Universitá di Pisa and CNISM, Largo Pontecorvo 3, 56127 Pisa, Italy*
[5]*Istituto Nazionale di Ottica, INO-CNR, U.O.S. Pisa "Adriano Gozzini," via Moruzzi 1, 56124 Pisa, Italy*

(Received 1 November 2012; revised manuscript received 25 August 2013; published 30 September 2013)

We propose a source for high-brightness ion and electron beams based on the ionization of an effusive atomic beam which is transversely laser cooled and compressed. The very low transverse temperature (mK range) and the relative low density of the starting atomic sample ensure excellent initial conditions for obtaining bright and monochromatic charge sources. In contrast to the standard photoionization techniques used by similar sources, we utilize field ionization of Rydberg atoms. This approach allows a substantial reduction of the required laser power and copes differently with the problems of the energy spread created during the ionization process and of the stochastic space-charge effect. Theoretical modeling and prospective ideas of this emerging technology are given.

DOI: 10.1103/PhysRevA.88.033424 PACS number(s): 37.10.De, 32.80.Ee, 41.75.Ak, 67.85.−d

## I. INTRODUCTION

Well controlled, monochromatic, and spatially focused electron and ion beams are invaluable tools in many research fields such as semiconductor and material sciences, data storage, surface studies (imaging, lithography), and biology. They are also becoming increasingly related to the emerging nanotechnology industry, for instance, as highly localized fabrication or diagnostic tools [1,2].

Recently, experimental realizations of novel ion or electron sources based on the ionization of laser-cooled atoms have been reported [3–20] and have shown the potential of these new sources. Due to the low temperatures associated with laser cooling, the ion (or electron) beam originating from the cold sample has an extremely narrow angular spread. This means that ion or electron sources based on the ionization of cold atoms would have the ability to create very small focal spots with relatively strong currents. Up to now, all experimental realizations have been performed in a magneto-optical trap (MOT) using direct ionization of the atoms. This leads to some limitations, especially in terms of flux (i.e., ion-electron current) and, because of the presence of magnetic fields, used to confine the neutral particles.

In this paper, we shall present ideas to overcome these problems based on the high flux given by a transversely laser-cooled and compressed atomic beam which is excited into a Rydberg state and subsequently ionized in the presence of an electric field. With our method, currents in the 10 nA range are achievable but, as we will show, Coulomb repulsion between charges (space-charge effects) are likely to seriously reduce the beam brightness. Nevertheless, there are operating regimes (current, energy, spot, and time domains) where our system still represents an advancement with respect to existing ion and electron sources.

We shall briefly describe the current status of this ion- and electron-beam technology and of existing realizations. Finally, we detail our proposition on how to achieve some of the unique capabilities of these ultracold sources. We recall here the main expected advantages related to these sources as follows.

(i) The initial energy dispersion of a 100 $\mu$K MOT atomic source is in the 10 neV range; the same applies to the transverse energy dispersion of a laser-cooled atomic beam.

(ii) Available atomic species range from alkali and alkaline atoms to noncontaminant gases and other elements of technological interest.

(iii) Ionization produces ions and electrons, so a reverse voltage would transform an ion source into an electron source.

(iv) The beam current can be controlled in real time, up to the femtosecond level and down to the single-particle limit solely by varying the laser intensity.

(v) The high brightness of this source will allow strong focusing even at very low beam energies. This makes possible the manipulation and the control of particle interactions at the nanometer level with eV beam energy.

## II. CHARGED PARTICLE SOURCES AND DEVICES

In this section, we will briefly review the state-of-the-art of ion- and electron-beam devices as well as of their applications, based on both standard and cold atom technologies. The *brightness* $B$ of a beam provides a measure of how much current can be concentrated on a small spot and is defined as

$$B = I/(A\Omega), \tag{1}$$

where $I$ is the beam current, $A$ is the beam surface area, and $\Omega$ is the beam solid angle [21]. This is a simplified definition valid for uniform current density and uniform angular spread uncorrelated with the particle position. A more complete discussion on the brightness can be found, for instance, in the book by Reiser [22] or in Ref. [23]. In our calculations we will make use of the definition given in Ref. [24]. The reduced brightness, defined as

$$B_{\mathrm{red}} = B/U, \tag{2}$$

 

where $U$, the beam energy (usually expressed in eV), is a fundamental quantity that characterizes the ability to create a small focal spot with enough current to be useful. For a monoenergetic beam, it is an invariant along the beam path in the absence of aberrations and interactions between particles [23]. Another useful figure of merit of a particle beam is the *emittance*, defined as the product of the beam focus diameter with the angular spread. The brightness of a beam is given by the ratio between current and the product of the emittances in the two transverse axes.

TABLE I. Properties of state-of-the-art electron sources: beam density, emission current, source (cathode) size, reduced brightness, and energy spread.

| Gun | W | $LaB_6$ | Schottky | CFEG |
|---|---|---|---|---|
| Density ($nA\,nm^{-2}$) | $2 \times 10^{-5}$ | $2 \times 10^{-4}$ | 0.2 | 0.5 |
| Current ($\mu A$) | 200 | 80 | 200 | 5 |
| Size ($\mu m$) | 100 | 20 | $<1$ | $<0.1$ |
| $B_{red}$ ($A\,m^{-2}sr^{-1}V^{-1}$) | $10^5$ | $10^6$ | $10^7$ | $10^8$ |
| $\Delta V$ (eV) | 1 | 0.5 | 0.4 | 0.3 |

### A. Focused ion beams

A focused-ion-beam (FIB) system uses an ion beam to raster over the surface of a sample in a similar way as a scanning electron microscope. A FIB machine consists of the source, the focusing or accelerating column, the sample stage and, often, a device to simultaneously monitor the results of the process. The beam energy is typically 30 keV. At this energy, ion currents of 1 pA and 100 pA can be focused to spot sizes of 2.5 nm and 15 nm, respectively. In the latter case, the current density in the core of the beam approaches $2 \times 10^{-4}$ $nA/nm^2$ ($20\ A/cm^2$). FIB machines have many applications, including *in situ* cross sectioning and analysis of a fabricated device, specimen preparation for transmission electron microscopy, milling (where material is removed), gas-assisted chemical vapor deposition (where material is deposited), mask repair and micromachining, scanning ion microscopy, secondary ion mass spectrometry (where secondary ions are generated and collected as the beam is scanned), and lithography [25]. In standard FIBs, the source is typically a gallium liquid-metal ion source (LMIS), used for its high surface tension and low vapor pressure. It has one major drawback, namely contamination of the treated surfaces by $Ga^+$ is inevitable. Other LMIS are also available, such as gold, gold alloys (Au-Ge, Au-Si), indium, and bismuth. They are used for very specific applications and their diffusion is much more limited.

For several decades there has been much effort to develop noncontaminant ion sources instead of LMIS. In particular, it is worth mentioning gas field ion sources (GFIS) [26], such as the Carl Zeiss Orion nanoFIB [27], which can provide for example noble gas ion sources. Although they can attain very good brightness and small energy spread, stability and ease of use remain a concern. Their use as FIB sources is therefore limited. Other well established ion sources for FIBs with noble gases, hydrogen, and oxygen are the plasma sources. Their performances are very good when high currents (tens of nA) are required but, conversely, their focusing properties are fair. In general, what makes an ion source suitable for FIB applications is the ensemble of qualities such as the high brightness, the low-energy dispersion leading to chromatic aberrations, the long-lasting life, the reliability, and ease of use during operation.

### B. Electron beams

Similarly, electron sources are used in a wealth of research fields and application domains that often require ultimate spatial control combined with precisely defined and tunable acceleration energy, as in the case of the scanning electron microscopes (SEM). The standard electron sources can produce remarkable results, but brightness, stability, and energy monochromaticity are now regarded as the limiting factors [2]. The goal for the next generation of microscopes, which can be roughly seen as a 0.1 nm probe, energy spread approaching or below 100 meV and 1 nA current, will certainly not be reached with the standard electron sources such as tungsten filaments (W), lanthanum hexaboride ($LaB_6$) thermionic sources, Schottky thermoassisted field emission guns, or cold field emission guns (CFEG). In particular, as indicated in Table I, no reliable electron source with energy spread below 0.3 eV has been obtained for electron microscopy. Furthermore, in standard setups, the implementation of a monochromator to reduce the energy spread degrades the brightness and limits the spatial resolution to several tens of nanometers. State-of-the-art SEM microscopes, like the Magellan XHR SEM by FEI [28], are able to produce electron beams with tunable energy between 1 kV and 30 kV and resolution of the order of 0.9 nm. Lower energies are also possible (down to 50 V) but at the expenses of resolution.

The use of laser-cooled atoms, such as those produced in a magneto-optical trap at a temperature of tens of micro-kelvin and corresponding energy dispersion of only 1 neV, seems promising to solve this problem. In particular, very low landing voltages (1–100 V) are expected with good spatial and energy resolutions. Such low-energy electrons can be very useful to induce, control, orientate chemical reactivity, to initiate selective dissociative processes [29], or realize faster electron-beam chemical lithography [30].

Essentially, all standard ion or electron sources have very high emitter current densities (see Table I), which produce strong space-charge effects and degrade the energy spread. In contrast, cold atom sources, such as transversely cooled atomic beams, can have a flux higher that $10^{10}$ particles per second through a 100 $\mu$m spot [31]. If fully ionized, they would produce currents of $\sim$1 nA, but with very small current density ($10^{-10}$ $nA\,nm^{-2}$), reducing space-charge effects and associated energy spread degradation. Small energy dispersion added to the very low initial velocity arising from the cold temperatures obtained by laser cooling should lead to a source with unprecedented performance. Consequently, ion or electron sources based on laser cooling of atoms can have simultaneously lower emittance and higher brightness than conventional sources. While in standard sources the emittance is lowered by making the source as small as possible (tens of nm), in cold sources it is the angular spread to be drastically reduced, leading to a lower emittance. As we will show in

Sec. III D, these good expectations for cold sources are somewhat limited nevertheless by space-charge effects.

### C. Laser-cooling technology and magneto-optical trap sources

It is clear from the previous discussion that efficient ionization of laser-cooled atoms and subsequent extraction of charged particles will provide a bright source of ions (or electrons). Indeed, laser-cooling techniques can greatly increase phase-space density, defined as the number of particles within a given position and momentum region, of an atomic sample. On the other end, Liouville's theorem states that, without extra knowledge about the microscopic distribution of the particles, electrostatic or magnetic fields are not able to enhance the phase-space density or, similarly, the reduced brightness of a sample.

Atomic samples with $10^7$–$10^9$ atoms can routinely be trapped in magneto-optical traps (MOTs) at temperatures of some hundreds of $\mu$K. Further and more complex cooling can lead to lower temperature ($\mu$K) or even to quantum degeneracy (Bose-Einstein condensation). To date, the list of optically trapped stable elements includes all alkali metals, all noble gases in metastable states, all alkaline-earth elements, and several other elements: Cr, Er, Ag, Yb, Hg, Cd, Dy, and Tm (see Refs. [32–35] for the most recent achievements). Less demanding is the transverse cooling of an atomic beam which has been realized also with other atomic species such as Al, Ga, Fe, In [36–40] and is in perspective for Si, Tl and other atoms of interest for nanoscience, such as boron, phosphorus, and arsenic [41–44].

The idea that, by efficiently ionizing and extracting charged particles, ultracold atoms may become a source of ions or electrons started in 2003 with the theoretical suggestion to ionize cold atoms for nanotechnology purposes [45,46]. This proposition emerged from previous fundamental studies of ultracold plasmas realized either by direct laser photoionization [47] or by the technique, initiated at Laboratoire Aimé Cotton [48], of laser promotion to highly excited (Rydberg) states which eventually ionize [49]. It has been shown that, even when starting with motionless atoms, collisions and stochastic Coulomb interaction between closed neighbors increases the plasma temperature to $T_e \sim 10$ K for the electron and $T_i \sim 1$ K for the ions. Nevertheless, this is still at least two orders of magnitudes below the thousands of kelvin typical of conventional electron and ion sources. Based on this knowledge, more detailed proposals, by the group of J. McClelland at NIST (Gaithersburg, USA) [4,50,51], and by the group of O. J. Luiten and E. Vredenbregt, from the University of Technology in Eindhoven (Netherlands) [3,5,6,24,52,53], have confirmed that sources based on cold atoms could perform ground-breaking experiments. For example, the ion source, called magneto-optical trap ion source (MOTIS) by the NIST group and ultracold ion source (UCIS) by the Eindhoven group, has a potential reduced brightness higher than $10^7$ A m$^{-2}$sr$^{-1}$V$^{-1}$, as compared to the best FIB with a measured reduced brightness of $10^6$ A m$^{-2}$sr$^{-1}$V$^{-1}$. In 2007 a group of the Lawrence Berkeley National Laboratory proposed another type of source based on a beam of neutral alkali-metal atoms excited in a pulsed mode where on average only one electron per pulse is generated [54]. Such a "Rydberg photocathode" source would deliver a sub-pA current, but should achieve an emittance and brightness approaching the quantum limit.

Then, NIST and Eindhoven groups reported results of their experiments [4,5]. These are based on near-threshold photoionization of a laser-cooled and trapped atomic gas. Using an extraction field of $\sim 1$ kV/cm with $\sim 1$ $\mu$s rise time, a preliminary ultracold plasma extraction experiment had been realized, showcasing the low emittance, even if not yet comparable with the state-of-the-art LMIS [3,52]. Later, a similar extraction of ions was realized with an average energy as low as 1 eV and an energy dispersion of 0.02 eV [3]. This value is to be compared with the several hundreds of meV obtained by standard sources for electrons, or even a few eV for the liquid metal ion source. These results were limited to pulsed sources and to low currents (tens of pA). More recently, the US team has expanded the capabilities of their focused-ion-beam system by demonstrating nanoscale focusing of low-energy chromium and Li ions (between 0.5 and 3 keV) [8,16]. Using time-dependent electric fields, the Eindhoven team reported in Ref. [12] an ion source temperature as small as 1 mK. They were able to control the phase-space distribution of the ion beam, creating new possibilities to correct the spherical and chromatic aberrations that presently limit their spatial resolution [10,11]. Recently, an Australian group joined the community showing impressive spatial shaping capability by producing arbitrarily shaped high-coherence electron bunches from cold atoms [14,17]. All this activity explains why the US company FEI and the French company Orsay Physics, are involved in collaboration with NIST and Eindhoven groups (for FEI) and with the French authors of this article (for Orsay Physics). If such a source became a real industrial prototype, it would offer perspectives for new and potentially impressive applications. Moreover, it would be the first time that "laser cooling" techniques lead to real industrial development [55]. We would also like to mention a complementary technique, based on extraction of laser-cooled trapped ions, which has been developed by K. Singer's group at Ulm (Germany) [9,56]. Competing with techniques based on scanning tunneling microscopy (STM), or on pierced AFM tips, this method should allow precise control of the amount and of the positioning of an ion at very low energies ($<1$ keV). Potential applications of this source include the fabrication of scalable solid-state quantum computers and deterministic doping, which is critical for the advancement of nanoelectronics. This method works for almost all chemical elements, but is slow, with a rate similar to what is possible to realize ($\sim$10 Hz) with on-demand schemes for particle delivery based on laser-cooled atoms [57].

## III. HIGH-FLUX COLD BEAM SOURCES

The use of standard magneto-optical traps as laser-cooled setups lead to some limitations: in terms of brightness, because of the limiting density and temperature in a MOT [24], of flux, because of the relatively small flux of incoming trapped atoms ($10^9$ atoms/s typically, corresponding to $\sim$100 pA), of static fields, because of the presence of magnetic field to confine the neutral particles, and of geometrical constraints, because of the several laser beams required to produce a MOT. A source

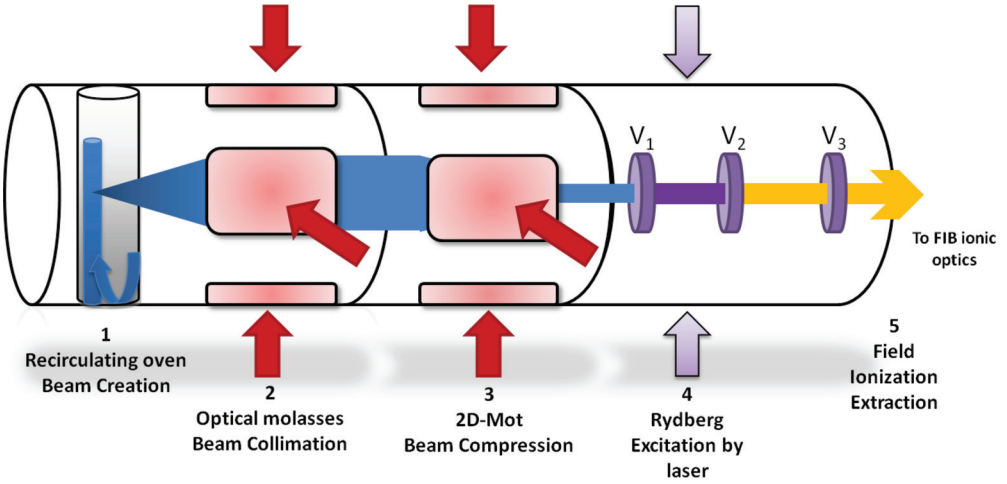


FIG. 1. (Color online) Sketch of the ultracold electron-ion source. An intense effusive atomic beam is transversely cooled and compressed using laser-cooling techniques. Electrons or ions (depending on electrode polarities) are produced by laser excitation to Rydberg states that are then field ionized. The beam is finally focused and accelerated, for instance, in a FIB column.

based on a high-flux atomic beam could overcome some of these limitations. Indeed, very recently, the NIST group [58] reported measurements and modeling of an ion source based on a laser-cooled atomic beam. They already demonstrated a total current greater than 5 nA and they predict that they could focus a 1 pA beam into a spot smaller than 1 nm. Although we cannot expect to have lower emittance than a MOT, the constraints on flux, magnetic field, and on geometry can be reduced. We will describe now some ideas towards the experimental realization of such a source. This source starts with the realization of a sufficiently cold and dense laser-cooled atomic beam with a large number of atoms, followed by an efficient laser ionization process. Success requires several ingredients, which have to be carefully tackled, as follows.

(1) A sufficiently "good" atomic source in terms of flux, density, number of atom, and energy dispersion.

(2) Efficient ionization process to create a bright monochromatic source.

(3) Extraction optics that do not degrade the properties of the source.

(4) Beam transport optics that do not degrade the properties of the beam.

(5) Efficient coupling with existing experiments and realization of industrial prototypes.

The effusive oven aimed to produce a high-flux atomic beam and, from that, a bright ion-electron source is sketched in Fig. 1. The beam is transversely laser cooled to sub-millikelvin temperature and compressed, for instance, in a magnetic quadrupole field to a sub-millimeter diameter [59], which increases the brightness of the atomic beam by several orders of magnitude [60]. High densities could be obtained directly after the effusive oven, without bothering for laser cooling and compressing the beam. Nevertheless, in this case the brightness would be substantially lower because of the residual divergence of the effusive beam.

To produce an electron or ion beam, we propose a method for the ionization and extraction, based around laser promotion of atoms to highly excited (Rydberg) states. The excited atoms from the atomic beam will then enter a region of slightly higher electric field where they are field ionized. We notice that the atomic ionization by way of Rydberg excitation has already been used in both an effusive atomic beam [61] and for cold atoms [3] but not with the scheme discussed below.

### A. Atomic source

Because laser cooling of cesium is well known in our laboratory [62] and because of its very good secondary ion mass spectrometry (SIMS) capability, we choose to develop a cesium beam. In order to have a compact and already almost-collimated beam, we choose a recirculating oven design (Ref. [63]). Recirculating ovens are more demanding than standard effusive ovens but have the great advantage that the effused element usage is minimized so, in principle, it need only be reloaded after thousands of hours of operation [64]. Briefly, the oven is composed of a candlestick that is inside a larger reservoir containing the cesium (see Fig. 2). The candlestick is heated at high temperature while the reservoir is kept just above the melting point of the cesium. Liquid cesium can get to the head of the candlestick through a wick and it is

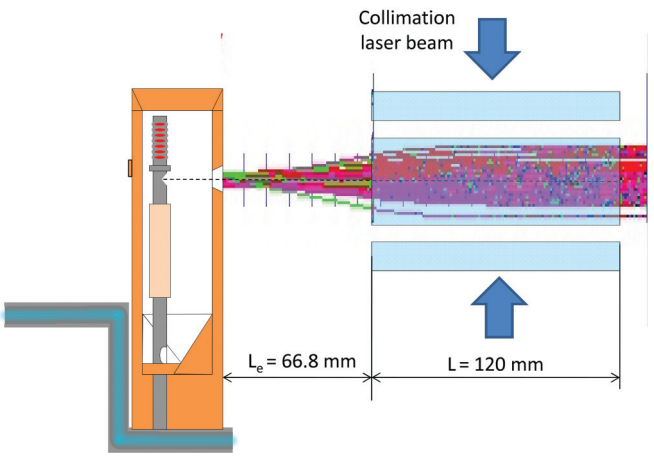


FIG. 2. (Color online) Simulations of the collimation of the Cs atomic beam after being emitted from the recirculating oven.

TABLE II. Characteristics of the "useful" atomic beam in the different region of the apparatus as shown in Fig. 1. The final flux $2 \times 10^{12}$ atoms/s corresponds to a current of roughly 300 nA.

| Region | 1 | 2 | 3 | 4–5 |
|---|---|---|---|---|
| Divergence (mrad) | 43 | 0.1 | 0.1 | 0.1 |
| Flux (atoms/s) | $2 \times 10^{14}$ | $5 \times 10^{13}$ | $5 \times 10^{13}$ | $2 \times 10^{12}$ |
| Diameter (mm) | 2 | 10 | 1.5 | 1 |
| Energy spread (meV) | 52 | 52 | 52 | 500 |

effused from there. A hole in the reservoir wall allows a small part of the effusive beam from the candlestick to come out while the greater part can flow back and be recirculated.

The flux increases with the oven temperature, but similarly the longitudinal mean velocity also increases with temperature, making the transverse laser cooling harder. Thus there is an optimal temperature for the oven. In the following, we choose to study the case of an $\sim$182 °C (455 K) cell creating a flux of Cs atoms as high as $2 \times 10^{14}$ per second, with few tens of milliradians divergence, a mean velocity of $\sim$317 m/s, and a transverse energy spread (FWHM) of 50 meV [63].

### B. Control of the atomic source: Laser cooling and compression

Collimation and compression of an atomic beam has already been well studied in our laboratory [65], as well as by several other groups (for example, Refs. [60,66,67]).

In this proposal, we study the collimation and then the compression of our source in two distinct zones, but clearly a single zone may also work and would actually simplify the experimental setup. Two-dimensional (2D) transverse laser cooling is performed using four beams. A very long cooling zone allows complete cooling but this would require very intense lasers. As a compromise we have designed a first collimation zone 12 cm long. In order to be close to the saturation intensity and using our experimentally available power (of 20 mW per beam) we choose the lasers to have an ellipsoidal shape of 1 cm $\times$ 12 cm. In order to give realistic values for what can be expected for our source, we have simulated this cooling using a simple Doppler cooling code [68] using a realistic model for the Cs atom. From the simulation, we optimized the detuning of each beam to be half of the natural linewidth of the atomic transition [$6s(F = 4) \rightarrow 6p_{3/2}(F' = 5)$]. We would like to mention that experimentally both sub-Doppler and strong-field effects have been observed to enhance the cooling process [65,69]. Thus the theoretical values we give are in fact quite conservative and it should be possible to have greater values in a real experiment. From the simulation, we end up with a collimated (divergence <0.5 mrad) beam of $5 \times 10^{13}$ atoms per second. Some trajectories are displayed in Fig. 2 and the results are summarized in Table II. Due to mechanical constraints the source is actually at 67 mm from the cooling stage, but a future design with a closer cooling stage is under consideration. Because the fastest atoms move too quickly to be cooled, only transverse velocities of atoms below 200 m/s are well collimated. This results in a collimated flux which is reduced by a factor 10 compared to the initial flux. However, higher velocity atoms are also naturally collimated, as most of them present a small divergence angle.

Simulation of the compression has also been performed in a very similar way. For instance, with a two-dimensional quadrupole magnetic-field gradient of 1 mT/cm and a 20-cm-long zone, the theoretical result is impressive, with an atomic beam not only cooled but also compressed to a very small radius. However, the model does not take into account losses due to collisions, which limits the experimental density. Estimating the maximum possible compression of an atomic beam in a nonuniform magnetic field and effect of transverse sub-Doppler cooling and compression is not easy. A limitation of an atomic beam density to a value on the order of $10^{12}/\text{cm}^3$ has been proposed [70], but we shall be more conservative here and take densities reached in a MOT, i.e., a density of cold atoms of nearly $10^{11}$ atoms per $\text{cm}^3$. This constrains the beam diameter to be roughly 1.5 mm [59,71]. Taking this limit as a more realistic value and a transverse temperature of 15 $\mu$K, which is easily achieved using sub-Doppler effects, lead to results that are summarized in Table II. Before ionization, for realistic parameters we predict an atomic flux of $5 \times 10^{13}$ atoms per second, with a 200 m/s axial velocity, and a divergence of only 0.15 mrad in a 1 mm beam radius.

### C. Control of the atomic ionization: Rydberg excitation and field ionization

To produce a useful charged particle beam, the atomic beam has to be ionized without degrading the low-temperature properties of the source, i.e., without increasing the energy spread and the transverse temperature of the charged particles

Typically, strong extraction fields (>1 kV/cm) are used to reduce the particles' transport time and thus damp the harmful effects of Coulomb interactions [24]. This leads to important limitations if using the direct photoionization technique. One problem arises from the differential voltage: even with very small 10 $\mu$m laser ionization zone, an extraction field value of 1 kV/cm already creates an energy dispersion of 1 eV, which is not much better than standard sources. Another problem is that nearly 10 W of continuous laser power is needed to efficiently photoionize an atomic beam [72]. Without an extra optical cavity, 10 W is really at the edge of the current industrial laser capability. In order to solve both problems, we propose to use field-ionized Rydberg atoms [73], rather than direct photoionization.

The main principle of the scheme exploits the fact that Rydberg states ionize at a very specific electric field: of $\sim 400 \times (\frac{30}{n})^4$ V/cm for alkali-metal atoms. Consequently, a well-conceived electric-field configuration should allow all Rydberg atoms to be ionized at nearly the same voltage producing a very monochromatic beam. Furthermore, the cross section for excitation to a Rydberg state is higher than the one required to photoionize the atom, by a factor of the ratio between the energy-level spacing ($n$ to $n + 1$) and the laser linewidth [73]. Thus, compared to the direct photoionization, the laser power needed is reduced by a factor $10^4$ for $n = 30$ and a 10 MHz linewidth laser. This means that only hundreds of milliwatts of continuous laser power are required to convert an atomic beam into Rydberg states.

The idea to laser promote to Rydberg with subsequent instantaneous field ionization at a given voltage looks interesting. Nevertheless, several details have to be studied, including the following.

(i) The efficiency of the Rydberg excitation.

(ii) The effect of the limited Rydberg lifetime before the field ionization.

(iii) The effect of the noninstantaneous Rydberg ionization.

(iv) The effect of an electric-field gradient.

To achieve the greatest possible current, laser promotion to highly excited (Rydberg) states will have to occur at high efficiency for the entire beam. Near 100% excitation efficiencies are possible using coherent excitation schemes [75,76], but we shall be more conservative here and assume only a 10% excitation probability with incoherent excitation. In fact, high excitation efficiencies would probably be prevented by a dipole blockade effect created by the fact that Rydberg state energies are shifted out of resonance by their dipole-dipole interaction with neighbors [77]. Furthermore, we would like to avoid high densities of Rydberg atoms which create a force between atoms, leading to motions that can degrade the brightness of the beam, as well as create a plasma [49,78,79]. Hence our aim is simply to reach a Rydberg density of few $10^{10}$ atoms/cm$^3$. We do not detail here the lasers we are going to use to ionize the cesium atoms but one simple solution would be the continuous ionization procedure already used in our team for Rydberg experiments [78]. In that case, after the 852 nm cooling laser, we used a 10 mW diode laser at 1470 nm followed by a (780 nm) Ti:sapphire laser. With such a laser focused to a diameter of 1000 $\mu$m, the transfer to the Rydberg state easily occurs within 500 ns [80], that is to say, well before the $\sim$ 200 m/s atoms leave the interaction zone. To ensure the atomic energy levels are not shifted out of resonance, an electric field homogeneous over the excitation volume is required.

After excitation, atoms have to travel until the point where they are field ionized. Fortunately, the radiative lifetime of $n\ell$ Rydberg states ($\ell$ being the orbital angular momentum of the valence electron) is long, on the order of several microseconds. A useful very simplified formula to estimate the lifetime in zero field is [78,81] $n^3(\ell+1/2)^2\times 10^{-10}$ s. This formula does not include the blackbody effect [82] which, for a temperature $T$, increases the decay rate by roughly $2\times 10^7\frac{T}{300\ \mathrm{K}}\mathrm{n}^{-2}(\mathrm{s}^{-1})$ [83]. In electric field the $\ell$ values are mixed and the lifetime is modified, but taken the conservative value of a pure $ns$ state, a typical state with $n=30$ as a lifetime on the order of 10 $\mu$s. With a beam velocity of 200 m/s the atoms can travel roughly 2 mm before decaying. In the proposed scheme atoms, during their travel, will see a higher and higher electric field until they reach the ionization point.

Looking at a typical Stark map (Fig. 3), we see that when the field increases, several avoided crossings between the Stark levels occur. As a consequence, the field-ionization rate of the Rydberg atoms would depend on the rising speed of the electric field up to the classical ionization limit. In order to minimize this effect, we suggest excitation to a Rydberg state at an electric field just below the classical ionization limit.

Another difficulty arises from the fact that Rydberg atoms do not instantaneously ionize at a definite electric-field value. In fact, the ionization effect is a tunneling phenomenon and is not so abrupt in an electric field as we have suggested. Rydberg atoms are ionized at an increasing rate as the electric field increases. Because the voltage at which atoms are ionized is proportional to the position of the atoms along the beam, creating a very monoenergetic ion (or electron) beam requires the atoms to ionize at the same longitudinal position. Because of the beam velocity, this means that the atoms have to be ionized very quickly, and thus the electric field $E$ must thus increase rapidly in space.

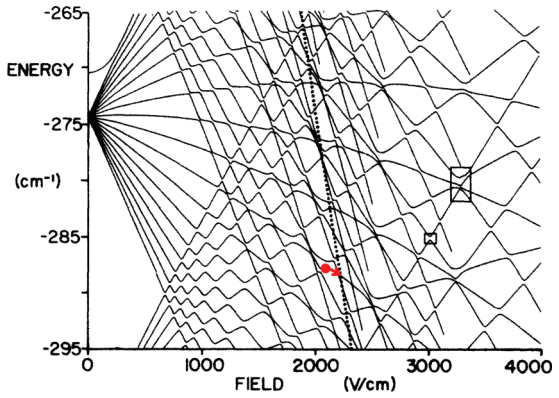


FIG. 3. (Color online) Energy levels of the sodium Rydberg state $n=20,\ell>1$ versus the electric field [74]. The dotted line is the classical ionization limit. The position of two stabilized states are shown in the two boxes. The red dot indicates a possible excitation zone and the arrow a typical path toward ionization.

In order to estimate the required electric-field gradient $E'$, we take the formula for the ionization rate $\Gamma[E]$ for a hydrogen atom [84] and consider the simple case of $v=200$ m/s atoms entering an ionization field region where a constant electric-field gradient $E'$ is present. We calculate the ionization probability $P(z_0+vt)=e^{-\int^t\Gamma[E(z_0+vt')]dt'}$ of the atoms along their trajectories. We then extract the distance $\Delta z$ between an ionization probability of 0.2 and 0.8. The resulting energy dispersion $\Delta V$ is shown in Table III. These results correspond to the so-called "red" ($m=0,n_2=n-1$ [84]) states of the hydrogen atom, but we have checked that the result is not crucially dependent on the chosen state. Obviously a more detailed model for cesium would be required, but the qualitative behavior will not be modified. It is also possible to take into account the velocity dispersion of the neutral atomic beam, but the results are affected by less than a factor 2, and thus we neglect this effect.

As expected, a very large gradient is needed in order to preserve a good monochromaticity. This leads to experimental constraints in the electrode design. We finally note that this problem can be reduced by using "exceptional" Rydberg states which, due to crossing or interference effects, ionize faster that standard ones. Unfortunately, for Cs almost no experimental study of such states exists. Based on a crude estimation using such an existing state (two of them are shown for Na in Fig. 3) [85–87] leads to an improvement of a factor 10 for the energy dispersion. It means that use of these special Rydberg states would result in a dramatic improvement of the characteristics of our source.

TABLE III. Effect on beam chromaticity of the ionization of the Rydberg levels. $\infty$ indicates direct photoionization, just above the threshold. $E_0$ is the ionization field, $E'$ the electric-field gradient, $\Delta z$ the spatial ionization length, $\Delta V$ the resulting energy dispersion, $\Delta V_{\text{curve}} = (3r^2/8)E'$ (for $r = 100\ \mu$m) is the energy dispersion due the transverse field gradient, and $\Delta V_{\text{photo}} = w_0 E_0$ (where $w_0 = 10\ \mu$m is the waist of the ionization laser) the energy dispersion in the case of direct photoionization. The state 30*e* is an exceptional one (see text).

| $n$ state | $E_0$ (kV/cm) | $E'$ (kV/cm/cm) | $\Delta z$ ($\mu$m) | $\Delta V$ (V) | $\Delta V_{\text{curve}}$ (V) | $\Delta V_{\text{tot}}$ (V) | $\Delta V_{\text{photo}}$ (V) |
|---|---|---|---|---|---|---|---|
| $\infty$ | 1 | | 10 | 1 | | 1 | 1 |
| 100 | 0.006 | 0.1 | 5 | 0.003 | 0.00375 | 0.00675 | 0.006 |
| 50 | 0.1 | 1 | 14 | 0.1 | 0.0375 | 0.138 | 0.1 |
| 40 | 0.24 | 10 | 4 | 0.1 | 0.375 | 0.475 | 0.24 |
| 30 | 0.7 | 1 | 140 | 10 | 0.0375 | 10 | 0.7 |
| 30 | 0.7 | 10 | 15 | 1 | 0.375 | 1.38 | 0.7 |
| 30*e* | 0.7 | 10 | 1.5 | 0.1 | 0.375 | 0.475 | 0.7 |
| 30 | 0.7 | 100 | 1.5 | 0.1 | 3.75 | 3.85 | 0.7 |
| 20 | 3.5 | 100 | 10 | 3 | 3.75 | 6.75 | 3.5 |
| 10 | 45 | 100 | 160 | 500 | 3.75 | 504 | 45 |

A steep gradient leads to other complications, such as the production of forces on Rydberg atoms, but this is negligible [88,89]. Moreover, the longitudinal field gradient leads, by Gauss's law, to a radial field gradient and thus to a curvature of equipotential lines and to a lens effect, as shown in Fig. 4. This has two consequences: first, an increase of the energy spread and, second, the formation of a crossover somewhere downstream on the beam, also visible in Fig. 4. The first arises because, even if the atoms are all ionized at the same field $E_0$, depending on their distance from the axis $r$, they are not ionized at the same voltage. Indeed, using first-order expansion of the voltage and of the field in cylindrical geometry, i.e., $V(z,r) \approx V(z,0) - V''(z,0)r^2/4$, we find that $\Delta V = (3r^2/8)E'$. This strongly limits the possible field gradients. For instance, with $r = 0.1$ mm a beam with only $\Delta V = 0.4$ V would require $E' \sim 10$ kV/cm/cm. Combined with the effect of the noninstantaneous ionization given in Table III this would lead, for $n = 30$, to a beam with 1 eV energy dispersion, which is not negligible, but is already a factor 5 better than standard FIBs. The last two columns of Table III compare the energy spread for the Rydberg ionization scheme with standard photoionization. For this comparison we made a "worst case analysis" by considering a longitudinal beam waist $w_0 = 10\ \mu$m for the ionization laser, and the value $r = 100\ \mu$m for the radial extension of the Rydberg excitation, producing large energy spreads for the largest field gradients. In Refs. [4,5] the authors used respectively 10 and 32 $\mu$m ionization laser waists for very low ion currents. Table III shows that the Rydberg ionization scheme is in general worse than direct photoionization unless for high $n > 40$ Rydberg states or for exceptional ones. For low currents it is reasonable to consider such small ionization waists, but to attain large currents, larger waists (and laser powers) are required. Thus we can conclude that for high current, where high acceleration would be required to avoid Coulomb effect, Rydberg excitation is better to have an energy spread which is competitive with LMIS ones. Also at low current, or low-energy (acceleration) beam, Rydberg excitation can lead to an energy spread improvement as compared to the direct photoionization scheme but one has to properly choose the target Rydberg state, using either high $n$ values or exceptional (but surely existing) Rydberg states.

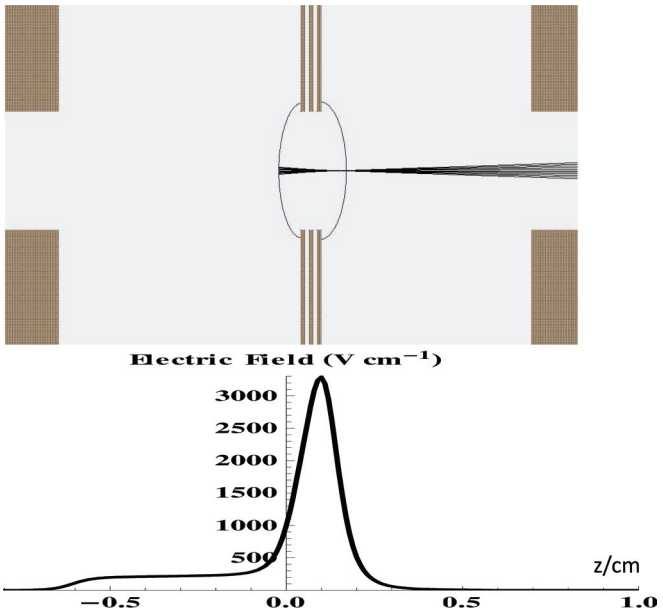


FIG. 4. (Color online) Electrodes (with cylindrical symmetry with internal diameter of 3 mm) and axial electric field (picture from Simion software). The voltages from left to right, 789, 493, 325, 45, and 45 V, have been chosen to illustrate the $n = 30$ case where a 1 kV/cm field and a 10 kV/cm/cm gradient is needed. The two curved lines are equipotential.

To conclude, the requirements on the electrodes to produce a monochromatic beam from Rydberg atoms are stringent, requiring an excitation zone of uniform electric field (almost no gradient) then, 2 mm later, a zone with a high gradient. A possible realization, simulated using Simion software, is proposed in Fig. 4. The fast modification of the gradient is achieved with three thin electrodes separated by only 300 $\mu$m. In order to avoid arcing, the geometry never creates an electric field higher than 100 kV/cm in vacuum, nor higher than 10 kV/cm on insulating (ceramic) arc length [2]. Other electrodes can be used for postacceleration and to control the extra fields necessary to avoid creating spherical and chromatic aberrations. Moreover, these will be strongly reduced by the high reduction ratio focusing lens that will be present in the focusing column.

### D. Charges extraction: Space-charge effects on the energy spread

The performances of any proposed charge source will eventually be limited not only by the initial density and temperature of the plasma but also by the ability to extract charges. During the latter phase, space-charge effects due to Coulomb explosion may degrade the characteristics of the ion and electron beams. Space-charge effects will appear ubiquitously, for instance, in cold atom sources based on photoionization and on Rydberg field ionization. In this section we will evaluate these effects for our source.

For ions, results from the NIST and Eindhoven groups show that, at least for low ion currents, even by using weak electric fields in the V/cm range, it is possible to reduce these effects and to have a very monochromatic ion beam [5,15,24].

For electrons, photoionization or field ionization of laser-cooled rubidium atoms shows a transverse temperature down to 10 K (1 K $\approx$ 0.086 meV) [7]. It is not clear if from an atomic beam the situation might be different and if in our setup lower electron temperatures can be achieved. By a careful control of residual electric and magnetic fields and by using low field acceleration out of a laser ionized atomic beam, an experiment from Hartmut Hotop's group (Kaiserslautern, Germany) shows a very high monochromaticity (10 meV) for a 100 pA electron current [72]. In such experiments (see also [90–93]), the atomic beam is not laser cooled, but the charged extraction problem should be similar to our experiments using cold atoms. From Ref. [72], where they analyzed the energy broadening due to the photoion space-charge effect, we may expect an energy broadening of the electron distribution given by

$$\Delta V_{\text{electron}} \sim 16\ \text{meV/nA}. \tag{3}$$

This formula does not include possible broadening effects associated with electric fields needed to extract the electrons and thus may be regarded as a lower limit for the given geometry when using the photoionization technique.

One conclusion that can be drawn from these experimental findings is that at low ion ($\leqslant$1 pA) and electron ($\leqslant$100 pA) currents, space-charge effects during the extraction do not limit the new source's performances. However, it would be important to have the possibility to attain large currents for integration reasons, in order to keep the experimental time as short as possible.

Consequently, it would be important to increase the beam current without creating too much chromatism or degrading the brightness. This may result difficultly because the differential voltage problem mentioned previously requires the use of a small electric field. On the other hand, the space-charge effects that dominate at large currents require a large electric field in order to reduce the interaction time and the Coulomb explosion. We will analyze here the case with our ionization scheme that proceeds through Rydberg states.

To model the space-charge effect within our accelerator we have performed numerical simulations using the general particle tracer (GPT) code taking into account all pairwise Coulomb interactions. We found it difficult to simulate the full (electron and ion) plasma because of complicated orbits of electrons around the surrounding ions. Therefore, we simulate only a given type of particles. This is clearly a bad approximation for electron beams because, as mentioned in Ref. [72], the electron energy broadening is also due to the field created by the ions. Indeed, ions are moving slowly and create stray electric fields that affect electrons. Fortunately, the experimental results summed up into Eq. (3) already give the final result. Therefore, to perform simulations for electrons, we start with an electron energy distribution matching the results of Eq. (3). For instance, for a 10 pA beam we create the initial distribution with an axial size $\sigma_z E = 0.16$ meV. Milli-eV energy resolution can be achieved in a weak extraction field, either by using direct photoionization or by using high ($n \approx 100$) Rydberg states (see Table III). Optimization of the spherical aberration of an optimal focusing lens is beyond the scope of this article and we have simulated only the very simple lens design shown on Fig. 5. As discussed previously it is not easy to predict the initial electron temperature. We thus have performed the simulation for temperature ranging from 10 K down to 1 mK. We define the spot size as the radius containing only half of the particles—those with the best focusing. Such a simple electrostatic lens already focuses the low (8 eV) energy beam on a small spot and with a small energy dispersion (3 meV). This is below the energy resolution required (typically <10 meV) to determine the vibrations of molecules on surfaces. The standard source for such experiments, as in high resolution electron energy loss spectroscopy (HREELS), uses a 10 pA current but focused only on 1 mm. Therefore, by allowing one to perform energy losses at high energy and high spatial resolution, our low-energy (0–20 eV) electron source can be very useful for investigation of vibrations of molecules, of surface structure, or of dispersion of surface phonons. It can also be used to induce, control, and orientate chemical reactivity, for instance, by initiating selective and efficient dissociative processes [29]. The realization of electron-beam chemical lithography using our source can therefore be much more precise and an order of magnitude faster than actually performed [30].

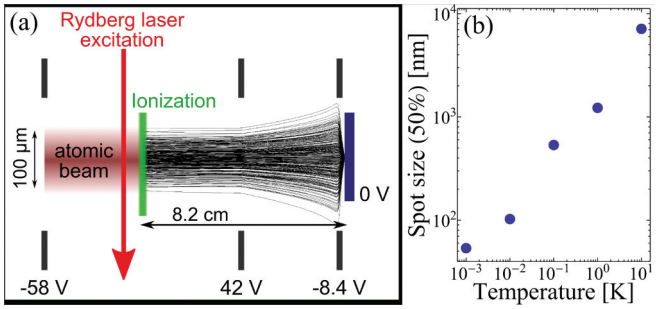


FIG. 5. (Color online) Simulation of a 10 pA electron beam produced by laser ionization of a sample of cold atoms. Left (a): trajectory simulation with electrodes of cylindrical symmetry with internal diameter of 2 mm. Right (b): spot size (for 50% of the beam particles) for several initial electron temperatures with an acceleration field of 12.5 V/cm.

It is difficult to predict what will be the reduced brightness of the source. Achieving very high brightness requires low electron temperature. However, one important point to remember is that, if the longitudinal energy spread does not enter in the brightness definition, only the transverse one does, the beam brightness is not constant in the presence of a

significant energy spread due to the buildup of a correlation of the transverse particle positions and the longitudinal particle momentum [94]. The chromatic aberration limits the spot diameter to $d_c = C_c\alpha(\Delta E/E)$, where $C_c$ is the chromatic aberration coefficient (generally on the order of 1 cm) and $\alpha$ is the convergence angle (generally not bigger than 10 mrad). Thus, even if the brightness of our source is not high, the focusing capability of this highly monoenergetic (small energy resolution $\Delta E$), low-energy electron is relatively high as shown by Fig. 5.

For an ion beam the situation is simpler to simulate. In fact, as the electrons move quickly, the electric field they create very rapidly disappears. Because of this, when simulating an ion beam their effects can be neglected. For the simulation we use the simplest possible electric-field configuration, namely a constant and homogeneous field, to study the evolution of the beam properties. This is not in contradiction with the field configuration described above (homogeneous + gradient) field as we are calculating here only the effects of the Coulomb interactions, the effects of the gradient on the energy spread being already evaluated in Table III. The only problem arises from the presence of the crossover present in Fig. 4 that, for very high currents, creates strong Coulomb effects. Nevertheless, it can be compensated and brought outside the region of interest by an appropriate choice of the electrode potentials. Furthermore, the use of exceptional Rydberg states will allow use of other electric-field configurations that should reduce this problem.

The starting point of the simulation is an ion beam with characteristics given in the last column of Table II and by the previous results. It is obviously not possible to simulate a continuous beam. Thus the simulation is performed using a limited number of particles. The flux of atoms, with 200 m/s axial velocities (100 m/s rms dispersion), is simulated by setting up to 40 000 particles with a Gaussian distribution of positions (100-$\mu$m-diameter and 1-$\mu$m-long zone). As shown in Table III, the 1-$\mu$m-long zone is achievable using a standard Rydberg state for an accelerated field of 1 kV/cm or by using an exceptional Rydberg state for higher fields. The 0.1 mm radial size was chosen in order to facilitate the laser excitation and to reduce any spherical aberrations in the following lenses. The uniform electric field varies in the range of 1–100 kV/cm. Results are shown in Fig. 6 where the transverse energy spread and the reduced brightness of the beam along its trajectory are plotted. Because the energy spread and brightness depend on the beam fraction (the radius) considered, we give results for the particles inside a phase-space volume containing half of the particles as explained in Ref. [24]. Clearly a high acceleration field is required in order to preserve a high brightness. But a large field would produce a too high longitudinal energy spread due to the voltage difference in the ionization area. On the other hand, Fig. 6 shows that the brightness reduces due to heating in the transverse plane even after the initial phase of acceleration, i.e., after few mm. As it is apparent from this figure, a general result is that only ion beams with less than 1 nA current are allowed without incurring into a dramatic decrease of the brightness.

In our simulations we also tested the influence of the initial distribution of charged particles, in particular, a random versus a uniform distribution of particles. It is known in fact that

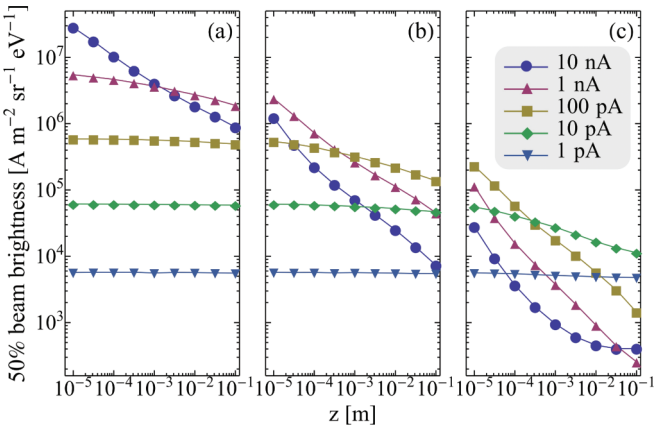


FIG. 6. (Color online) GPT simulations of the acceleration part for of an ion source of several different currents (1 pA–10 nA), with $\sigma_z = 1$ $\mu$m and $R = 50$ $\mu$m. The reduced brightness of the 50% "best" particles after an acceleration along $z$ created by uniform electric fields of 100 kV/cm (a), 10 kV/cm (b), and 1 kV/cm (c).

disordered-induced heating, or Boersch effect, due to random positioning of the charged particles, can have a large effect on the brightness [15,24]. This could be a real concern especially when using direct photoionization, while the use of Rydberg field ionization can help to solve this problem through the "Rydberg dipole blockade," i.e., the possibility to avoid laser excitation of close Rydberg neighbors [77,80,95–102]. Our simulation shows that, in our conditions using a sufficiently high number of particles, the results of Fig. 6 become only very slightly worse (less than a factor 2) when the atoms are randomly distributed.

We have checked that results for other initial beam diameters depend only on the current density. For instance, a 100 nA beam with a 1 mm diameter would lead to similar results as the 1 nA beam with a 0.1 mm diameter. For high acceleration fields the obtained reduced brightness can be similar or even greater than $B_{\mathrm{red}} = 10^6$ A m$^{-2}$sr$^{-1}$eV$^{-1}$ for a gallium LMIS.

### E. Coupling with existing setups and realization of industrial prototypes

One key feature of these sources based on cold atom ionization is the low-energy dispersion. This means that our monochromatic source can work at lower kinetic energies than 30 keV (standard for FIB) with similar performances, in contrast with the other sources which are degraded at lower beam energies. By fitting this source into an existing FIB column, this shall open the way to a generation of focused-ion-beam instruments.

Similarly, as "cold" electrons are also available after the ionization process, a "simple" voltage reversal should provide a bright electron source. With such a source we could manipulate and control particles with eV beam energy. Ultimately, for low currents at a very low beam energy, we can hope to focus on spots size close to the diffraction limit.

Finally, we note that although performances look very promising, the experimental realization is difficult. For instance, it is obvious that for the real apparatus the greatest care has to be taken during the instrument conception to provide

good alignment to the optical axis, good laser stability in terms of intensity, wavelength, and beam alignment, to make the instrument rigid, tolerant to room-temperature fluctuations. Equally important are the high stability of high voltage (HV) power supplies, of the external parameters including mechanical isolation, shielding of external fields, and room-temperature stabilization.

## IV. CONCLUSIONS

We have proposed an ion or electron source based on the field ionization of laser-excited Rydberg atoms created in a laser-cooled atomic beam. The apparatus is under construction in our laboratory. We have discussed in detail here all issues about laser cooling, excitation, and ionization. Moreover, we have studied the effects of inter-particle Coulomb interaction during charge extraction (space-charge effects) on the performances (brightness and energy dispersion) of the proposed source.

The proposed ion or electron source should allow for focusing of a very low-energy beam on a much smaller spot than previously achievable. Unfortunately, the effects due to space-charge interactions seem to severely limit the performances of our source for large currents. Nevertheless, the proposed source represents an improvement with respect to the existing standard source in a definite range of currents and beam energies. The method of going through Rydberg states is promising, as compared to the already used photoionization method, because it requires orders of magnitude less laser power and could in principle take care of the disordered-induced heating by using the Rydberg blockade effect. This Dipole-blockade technique may have other interests such as to allow the production of a fast and (quasi-)deterministic single ion or electron source [103]. The use of other ionization techniques such as rare-gas ionization with strongly focused synchrotron radiation combined with the penetrating field technique may be also useful to limit the differential voltage problem [93,104].

The improvement in terms of beam monochromaticity and the capability to focus low-energy ions or electrons on a small spot can be used to perform microscopy, spectroscopy, and lithography experiments with unprecedented resolution. High-energy resolution of the monochromatic sources can also superbly resolve molecular vibrational transitions, quasiparticles, or collective excitations and interaction effects due to the surrounding environment.

The possibility for a pulsed source would help to achieve an important goal in chemistry: find an imaging technique able to monitor the sequence of different configurations during a chemical reaction [105]. To achieve such high temporal resolution, several groups have realized ultrafast electron microscope or ultrafast electron diffraction, based on intense femtosecond laser-induced photoemission from a nanometer-sized tip [106,107]. Using femtosecond ionization, a source based on cold atoms should have superior qualities in terms of space-charge effects and energy resolution [6,7,19,20]. The laser control of the ionization process can also lead to production of deterministic single-ion implantation. Hence single-ion implantation of species featuring magnetic spin properties can be foreseen, leading to precise doping of materials for, e.g., spintronic applications, that is, the ability to manipulate electrical currents (ideally consisting of single electrons).

Finally, we mention that further improvements are still possible in terms of minimum achievable temperature, a more dense sample, or a higher atomic flux (for instance, using seeded supersonic alkali-metal atom beams). We hope that this study of ionization of a cold atomic beam will open the way to spectacular experimental realizations and to exciting theoretical studies.

## ACKNOWLEDGMENTS

We thank C. Colliex, M. Allegrini, A. Lafosse, and F. Robicheaux for helpful discussions. We are grateful to Bas Van der Geer for help with the use of the GPT software. The research leading to these results has received funding from Institut Francilien de Recherche sur les Atomes Froids (IFRAF), fédération de recherche Lumière Matière (LUMAT), the European Union Seventh Framework Program FP7/2007-2013 under Grant Agreement No. 251391 COLDBEAMS and from the European Research Council under Grant Agreement No. 277762 COLDNANO. A.F. has been supported by the *Triangle de la Physique* under Contracts No. 2007-n.74T and No. 2009-035T GULFSTREAM. N.Š. has been supported by Campus France with a "Bourse de stage d'approfondissement."

[1] E. L. Wolf, *Nanophysics and Nanotechnology: An Introduction to Modern Concepts in Nanoscience* (Wiley-VCH Verlag GmbH, Weinheim, 2008), p. 308.

[2] J. Orloff, *Handbook of Charged Particle Optics* (CRC Press, Boca Raton, FL, 2008).

[3] B. J. Claessens, M. P. Reijnders, G. Taban, O. J. Luiten, and E. J. Vredenbregt, Phys. Plasmas **14**, 093101 (2007).

[4] J. L. Hanssen, S. B. Hill, J. Orloff, and J. J. McClelland, Nano Lett. **8**, 2844 (2008).

[5] M. P. Reijnders, P. A. van Kruisbergen, G. Taban, S. B. van der Geer, P. H. A. Mutsaers, E. J. D. Vredenbregt, and O. J. Luiten, Phys. Rev. Lett. **102**, 034802 (2009).

[6] S. B. van der Geer, M. J. de Loos, E. J. D. Vredenbregt, and O. J. Luiten, Microsc. Microanal. **15**, 282 (2009).

[7] G. Taban, M. P. Reijnders, B. Fleskens, S. B. van der Geer, O. J. Luiten, and E. J. D. Vredenbregt, Europhys. Lett. **914**, 46004 (2010).

[8] A. V. Steele, B. Knuffman, J. J. McClelland, and J. Orloff, J. Vac. Sci. Technol., B: Microelectron. Nanometer Struct. **28**, C6F1 (2010).

[9] W. Schnitzler, G. Jacob, R. Fickler, F. Schmidt-Kaler, and K. Singer, New J. Phys. **12**, 065023 (2010).

[10] M. P. Reijnders, N. Debernardi, S. B. van der Geer, P. H. A. Mutsaers, E. J. D. Vredenbregt, and O. J. Luiten, Phys. Rev. Lett. **105**, 034802 (2010).

[11] M. P. Reijnders, N. Debernardi, S. B. van der Geer, P. H. A. Mutsaers, E. J. D. Vredenbregt, and O. J. Luiten, J. Appl. Phys. **109**, 033302 (2011).

[12] N. Debernardi, M. P. Reijnders, W. J. Engelen, T. T. J. Clevis, P. H. A. Mutsaers, O. J. Luiten, and E. J. D. Vredenbregt, J. Appl. Phys. **110**, 024501 (2011).

[13] A. J. McCulloch, D. V. Sheludko, S. D. Saliba, S. C. Bell, M. Junker, K. A. Nugent, and R. E. Scholten, Nature Phys. **7**, 785 (2011).

[14] E. Vredenbregt and J. Luiten, Nature Phys. **7**, 747 (2011).

[15] A. V. Steele, B. Knuffman, and J. J. McClelland, J. Appl. Phys. **109**, 104308 (2011).

[16] B. Knuffman, A. V. Steele, J. Orloff, and J. J. McClelland, New J. Phys. **13**, 103035 (2011).

[17] S. D. Saliba, C. T. Putkunz, D. V. Sheludko, A. J. McCulloch, K. A. Nugent, and R. E. Scholten, Opt. Express **20**, 3967 (2012).

[18] N. Debernardi, R. W. L. van Vliembergen, W. J. Engelen, K. H. M. Hermans, M. P. Reijnders, S. B. van der Geer, P. H. A. Mutsaers, O. J. Luiten, and E. J. D. Vredenbregt, New J. Phys. **14**, 083011 (2012).

[19] W. J. Engelen, M. A. van der Heijden, D. J. Bakker, E. J. D. Vredenbregt, and O. J. Luiten, Nat. Commun. **4**, 1693 (2013).

[20] A. J. McCulloch, D. V. Sheludko, M. Junker, and R. E. Scholten, Nat. Commun. **4**, 1692 (2013).

[21] C. A. Brau, in *What Brightness Means*, Proceedings of the ICFA Workshop. Held 1-6 July 2002 in Chia Laguna, Sardinia, Italy, edited by J. Rosenzweig, G. Travish, and L. Serafini (World Scientific, Singapore, 2003), pp. 20–27.

[22] M. Reiser, *Theory and Design of Charged Particle Beams* (Wiley-VCH, Weinheim, 2008).

[23] C. Lejeune and J. Aubert, Adv. Electron. Electron Phys. Suppl. A **13**, 159 (1980).

[24] S. B. van der Geer, M. P. Reijnders, M. J. de Loos, E. J. D. Vredenbregt, P. H. A. Mutsaers, and O. J. Luiten, J. Appl. Phys. **102**, 094312 (2007).

[25] J. Gierak, Semicond. Sci. Technol. **24**, 043001 (2009).

[26] N. V. Tondare, J. Vac. Sci. Technol. A **23**, 1498 (2005).

[27] http://www.youtube.com/watch?v=tu_vgh8zm-i or http://www.zeiss.de/c1256a770030bce0/webviewtopnewsalle/871d197f6a58a078c1257a7c00229140?opendocument.

[28] http://www.fei.com/products/scanning-electron-microscopes/magellan.aspx.

[29] C. R. Arumainayagam, H.-L. Lee, R. B. Nelson, D. R. Haines, and R. P. Gunawardane, Surf. Sci. Rep. **65**, 1 (2010).

[30] A. Lafosse, M. Bertin, and R. Azria, Prog. Surf. Sci. **84**, 177 (2009).

[31] P. Meystre, *Atom Optics*, Vol. 33 (Springer-Verlag, New York, 2001).

[32] K.-A. Brickman, M.-S. Chang, M. Acton, A. Chew, D. Matsukevich, P. C. Haljan, V. S. Bagnato, and C. Monroe, Phys. Rev. A **76**, 043411 (2007).

[33] S. De, U. Dammalapati, K. Jungmann, and L. Willmann, Phys. Rev. A **79**, 041402(R) (2009).

[34] S. H. Youn, M. Lu, U. Ray, and B. L. Lev, Phys. Rev. A **82**, 043425 (2010).

[35] D. Sukachev, A. Sokolov, K. Chebakov, A. Akimov, S. Kanorsky, N. Kolachevsky, and V. Sorokin, Phys. Rev. A **82**, 011405(R) (2010).

[36] R. W. McGowan, D. M. Giltner, and S. A. Lee, Opt. Lett. **20**, 2535 (1995).

[37] S. J. Rehse, K. M. Bockel, and S. A. Lee, Phys. Rev. A **69**, 063404 (2004).

[38] B. Smeets, R. W. Herfst, L. P. Maguire, E. T. Sligte, P. Straten, H. C. W. Beijerinck, and K. A. H. Leeuwen, Appl. Phys. B: Lasers Opt. **80**, 833 (2005).

[39] B. Klöter, C. Weber, D. Haubrich, D. Meschede, and H. Metcalf, Phys. Rev. A **77**, 033402 (2008).

[40] V. Balykin and P. Melentiev, Nanotechnol. Russ. **4**, 425 (2009).

[41] W. M. Fairbank, S. A. Lee, W. P. Czajkowski, and J. S. Kluck, in *A Laser-cooled Single-atom-on-demand Source for Si Quantum Computing*, edited by T. Ralph and P. K. Lam (AIP, New York, 2011), AIP Conf. Proc. No. **1363**, 173 (2011).

[42] I. Fan, T.-L. Chen, Y.-S. Liu, Y.-H. Lien, J.-T. Shy, and Y.-W. Liu, Phys. Rev. A **84**, 042504 (2011).

[43] AEGIS Collaboration. Antimatter experiment: Gravity, interferometry, spectroscopy: http://cdsweb.cern.ch/record/1037532. Technical report. http://cdsweb.cern.ch/record/1037532.

[44] H. Perrin, P. Lemonde, F. Pereira dos Santos, V. Josse, B. Laburthe Tolra, F. Chevy, and D. Comparat, C. R. Phys. **12**, 417 (2011).

[45] B. G. Freĭnkman, A. V. Eletskiĭ, and S. I. Zaĭtsev, JETP Lett. **78**, 255 (2003).

[46] B. G. Freinkman, A. V. Eletskii, and S. I. Zaitsev, Microelectron. Eng. **73**, 139 (2004).

[47] T. C. Killian, S. Kulin, S. D. Bergeson, L. A. Orozco, C. Orzel, and S. L. Rolston, Phys. Rev. Lett. **83**, 4776 (1999).

[48] M. P. Robinson, B. L. Tolra, M. W. Noel, T. F. Gallagher, and P. Pillet, Phys. Rev. Lett. **85**, 4466 (2000).

[49] T. C. Killian, T. Pattard, T. Pohl, and J. M. Rost, Phys. Rep. **449**, 77 (2007).

[50] J. L. Hanssen, E. A. Dakin, J. J. McClelland, and M. Jacka, J. Vac. Sci. Technol. B: Microelectron. Nanometer Struct. **24**, 2907 (2006).

[51] J. L. Hanssen, J. J. McClelland, E. A. Dakin, and M. Jacka, Phys. Rev. A **74**, 063416 (2006).

[52] O. J. Luiten, B. J. Claessens, S. B. van der Geer, M. P. Reijnders, G. Taban, and E. J. D. Vredenbregt, Int. J. Mod. Phys. A **22**, 3882 (2007).

[53] B. J. Claessens, S. B. van der Geer, G. Taban, E. J. D. Vredenbregt, and O. J. Luiten, Phys. Rev. Lett. **95**, 164801 (2005).

[54] M. Zolotorev, E. D. Commins, and F. Sannibale, Phys. Rev. Lett. **98**, 184801 (2007).

[55] K. Weatherill and E. Vredenbregt, Phys. World **25**, 38 (2012).

[56] W. Schnitzler, N. M. Linke, R. Fickler, J. Meijer, F. Schmidt-Kaler, and K. Singer, Phys. Rev. Lett. **102**, 070501 (2009).

[57] J. J. McClelland and S. B. Hill, Appl. Phys. Lett. **82**, 3128 (2003).

[58] B. Knuffman, A. V. Steele, and J. J. McClelland, J. Appl. Phys. **114**, 044303 (2013).

[59] H. J. Metcalf and P. van der Straten, *Laser Cooling and Trapping* (Springer, New York, 1999).

[60] M. D. Hoogerland, J. P. J. Driessen, E. J. L. Vredenbregt, H. J. L. Megens, M. P. Schuwer, H. C. W. Beijerinck, and K. A. H. van Leeuwen, Appl. Phys. B **62**, 323 (1996).

[61] T. Oomori, K. Ono, S. Fujita, and Y. Murai, Appl. Phys. Lett. **50**, 71 (1987).

[62] I. Mourachko, D. Comparat, F. de Tomasi, A. Fioretti, P. Nosbaum, V. M. Akulin, and P. Pillet, Phys. Rev. Lett. **80**, 253 (1998).

[63] A. Pailloux, T. Alpettaz, and E. Lizon, Rev. Sci. Instrum. **78**, 023102 (2007).

[64] L. V. Hau, J. A. Golovchenko, and M. M. Burns, Rev. Sci. Instrum. **65**, 3746 (1994).

[65] J. Yu, J. Djemaa, P. Nosbaum, and P. Pillet, Opt. Commun. **112**, 136 (1994).

[66] F. Lison, P. Schuh, D. Haubrich, and D. Meschede, Phys. Rev. A **61**, 013405 (1999).

[67] C. Slowe, L. Vernac, and L. V. Hau, Rev. Sci. Instrum. **76**, 103101 (2005).

[68] E. J. D. Vredenbregt and K. A. H. van Leeuwen, Am. J. Phys. **71**, 760 (2003).

[69] C. Valentin, M.-C. Gagné, J. Yu, and P. Pillet, Europhys. Lett. **17**, 133 (1992).

[70] V. I. Balykin and V. G. Minogin, J. Exp. Theor. Phys. **96**, 8 (2003).

[71] C. G. Townsend, N. H. Edwards, C. J. Cooper, K. P. Zetie, C. J. Foot, A. M. Steane, P. Szriftgiser, H. Perrin, and J. Dalibard, Phys. Rev. A **52**, 1423 (1995).

[72] J. Bmmels, E. Leber, A. Gopalan, J. M. Weber, S. Barsotti, M. W. Ruf, and H. Hotop, Rev. Sci. Instrum. **72**, 4098 (2001).

[73] T. F. Gallagher, *Rydberg Atoms* (Cambridge University Press, Cambridge, UK, 1994).

[74] P. McNicholl, T. Bergeman, and H. J. Metcalf, Phys. Rev. A **37**, 3302 (1988).

[75] N. V. Vitanov, T. Halfmann, B. W. Shore, and K. Bergmann, Annu. Rev. Phys. Chem. **52**, 763 (2001).

[76] T. Cubel, B. K. Teo, V. S. Malinovsky, J. R. Guest, A. Reinhard, B. Knuffman, P. R. Berman, and G. Raithel, Phys. Rev. A **72**, 023405 (2005).

[77] M. D. Lukin, M. Fleischhauer, R. Cote, L. M. Duan, D. Jaksch, J. I. Cirac, and P. Zoller, Phys. Rev. Lett. **87**, 037901 (2001).

[78] D. Comparat and P. Pillet, J. Opt. Soc. Am. B **27**, 208 (2010).

[79] Th. F. Gallagher and P. Pillet, Adv. At., Mol., Opt. Phys. **56**, 161 (2008).

[80] T. Vogt, M. Viteau, A. Chotia, J. Zhao, D. Comparat, and P. Pillet, Phys. Rev. Lett. **99**, 073002 (2007).

[81] M. W. Horbatsch, M. Horbatsch, and E. A. Hessels, J. Phys. B: At. Mol. Phys. **38**, 1765 (2005).

[82] I. I. Beterov, I. I. Ryabtsev, D. B. Tretyakov, and V. M. Entin, Phys. Rev. A **79**, 052504 (2009).

[83] J. W. Farley and W. H. Wing, Phys. Rev. A **23**, 2397 (1981).

[84] R. J. Damburg and V. V. Kolosov, J. Phys. B **12**, 2637 (1979).

[85] C. Chardonnet, D. Delande, and J. C. Gay, Phys. Rev. A **39**, 1066 (1989).

[86] D. A. Harmin, Phys. Rev. A **30**, 2413 (1984).

[87] A. König, J. Neukammer, H. Hieronymus, and H. Rinneberg, Phys. Rev. A **43**, 2402 (1991).

[88] N. Vanhaecke, D. Comparat, and P. Pillet, J. Phys. B **38**, S409 (2005).

[89] S. D. Hogan, D. Sprecher, M. Andrist, N. Vanhaecke, and F. Merkt, Phys. Rev. A **76**, 023412 (2007).

[90] A. Schramm, J. M. Weber, J. Kreil, D. Klar, M.-W. Ruf, and H. Hotop, Phys. Rev. Lett. **81**, 778 (1998).

[91] A. Gopalan, J. Bömmels, S. Götte, A. Landwehr, K. Franz, M.-W. Ruf, H. Hotop, and K. Bartschat, Eur. Phys. J. D **22**, 17 (2003).

[92] V. L. Sukhorukov, I. D. Petrov, M. Schäfer, F. Merkt, M.-W. Ruf, and H. Hotop, J. Phys. B: At. Mol. Phys. **45**, 092001 (2012).

[93] M. Kitajima, M. Kurokawa, T. Kishino, K. Toyoshima, T. Odagiri, H. Kato, K. Anzai, M. Hoshino, H. Tanaka, and K. Ito, Eur. Phys. J. D **66**, 130 (2012).

[94] K. Floettmann, Phys. Rev. Spec. Top.–Accel. Beams **6**, 034202 (2003).

[95] E. Urban, T. A. Johnson, T. Henage, L. Isenhower, D. D. Yavuz, T. G. Walker, and M. Saffman, Nat. Phys. **5**, 110 (2009).

[96] J. V. Hernández and F. Robicheaux, J. Phys. B: At. Mol. Phys. **41**, 195301 (2008).

[97] A. Chotia, M. Viteau, T. Vogt, D. Comparat, and P. Pillet, New J. Phys. **10**, 045031 (2008).

[98] M. Reetz-Lamour, J. Deiglmayr, T. Amthor, and M. Weidemüller, New J. Phys. **10**, 045026 (2008).

[99] C. Ates, T. Pohl, T. Pattard, and J. M. Rost, Phys. Rev. Lett. **98**, 023002 (2007).

[100] R. Heidemann, U. Raitzsch, V. Bendkowsky, B. Butscher, R. Löw, L. Santos, and T. Pfau, Phys. Rev. Lett. **99**, 163601 (2007).

[101] D. Tong, S. M. Farooqi, J. Stanojevic, S. Krishnan, Y. P. Zhang, R. Côté, E. E. Eyler, and P. L. Gould, Phys. Rev. Lett. **93**, 063001 (2004).

[102] T. Vogt, M. Viteau, J. Zhao, A. Chotia, D. Comparat, and P. Pillet, Phys. Rev. Lett. **97**, 083003 (2006).

[103] C. Ates, I. Lesanovsky, C. S. Adams, and K. J. Weatherill, Phys. Rev. Lett. **110**, 213003 (2013).

[104] M. Kurokawa, M. Kitajima, K. Toyoshima, T. Odagiri, H. Kato, H. Kawahara, M. Hoshino, H. Tanaka, and K. Ito, Phys. Rev. A **82**, 062707 (2010).

[105] W. E. King, G. H. Campbell, A. Frank, B. Reed, J. F. Schmerge, B. J. Siwick, B. C. Stuart, and P. M. Weber, J. Appl. Phys. **97**, 111101 (2005).

[106] B. W. Reed, M. R. Armstrong, N. D. Browning, G. H. Campbell, J. E. Evans, T. Lagrange, and D. J. Masiel, Microsc. Microanal. **15**, 272 (2009).

[107] C. Godbout and B. J. Siwick, Phys. Canada **65**, 75 (2009).